

The ‘Roxolany Tephra’ (Ukraine) – new evidence for an origin from Ciomadul volcano, East Carpathians

Sabine Wulf^{1,2*}, Stanisław Fedorowicz³, Daniel Veres⁴, Maria Łanczont⁵, Dávid Karátson⁶, Ralf Gertisser⁷, Marc Bormann⁸, Enikő Magyari⁹, Oona Appelt¹⁰, Ulrich Hambach¹¹, Petro F. Gozhyk¹²

¹ Senckenberg Research Institute and Natural History Museum, BIK-F, TSP6 Evolution and Climate, Senckenberganlage 25, D-60325 Frankfurt a.M., Germany

² Institute for Geosciences, University of Heidelberg, Im Neuenheimer Feld 234, D-69120 Heidelberg, Germany

³ University of Gdańsk, Institute of Geography, Department of Quaternary Geomorphology and Geology, ul. Bażyńskiego 4, 80-950 Gdańsk, Poland

⁴ Romanian Academy Institute of Speleology "Emil Racovita", Clinicilor 5, 400006 Cluj-Napoca, Romania

⁵ Department of Geoecology and Palaeogeography, Maria Curie-Skłodowska University, Al. Kraśnicka 2 cd, 20-718 Lublin, Poland

⁶ Eötvös University, Department of Physical Geography, H-1117 Budapest, Pázmány s. 1/C, Hungary

⁷ School of Physical and Geographical Sciences, Keele University, Keele ST5 5BG, United Kingdom

⁸ University of Cologne, Institute of Geography Education, Gronewaldstr. 2, D-50931 Cologne, Germany

⁹ Eötvös University, MTA-MTM-ELTE Research Group for Paleontology, Pázmány s. 1/C, H-1117 Budapest, Hungary

¹⁰ Helmholtz Centre Potsdam, GFZ German Research Centre for Geosciences, Section 4.3 Chemistry and Physics of Earth Materials, Telegrafenberg, D-14473 Potsdam, Germany

¹¹ BayCEER & Chair of Geomorphology, University of Bayreuth, D-95440 Bayreuth, Germany

¹² Institute of Geological Sciences, National Academy of Sciences of Ukraine, Gonchara 55B, 01 601 Kyiv, Ukraine

* **Corresponding author:** Sabine.Wulf@senckenberg.de (S.Wulf), facsimile +49-(0)6221-545503

Keywords: Tephra; Roxolany loess; Ukraine; Ciomadul; Lake St. Ana.

Abstract

We present major element glass data and correlations of the ‘Roxolany Tephra’ – a so far geochemically unconstrained volcanic ash layer previously described in last glacial (MIS2) loess deposits of the Roxolany loess-palaeosol complex in the SW Ukraine. This exceptionally well preserved, 2-3 cm thick tephra layer is characterised by a rhyolitic glass composition that is comparable to that of proximal tephra units from Ciomadul volcano in the East Carpathians, central Romania. The chemistry particularly matches that of the final LSPA pyroclastic fall unit of St. Ana crater that is radiocarbon dated in the proximal Mohoš coring site (MOH-2) at 29.6 ± 0.62 cal ka BP. The age of the tephra correlative is in agreement with the newest radiocarbon and IR-OSL age constraints from overlying palaeosols and tephra-embedding loess of the Roxolany sequence, respectively, which place the tephra between ca. 33 and 24 cal ka BP, and thus confirm the long-debated chronostratigraphy of this important

environmental archive. The occurrence of a distal Ciomadul tephra ca. 350 km east of its source indicates a great potential of further tephra and cryptotephra findings from this volcanic complex in the south-eastern Mediterranean and Black Sea region.

1. Introduction

The loess-palaeosol complex near the village of Roxolany in the SW Ukraine (Fig. 1) provides an almost complete Pleistocene terrestrial sedimentary record and is therefore the most representative sequence for the reconstruction of long-term palaeoclimatic and environmental changes in the Northern Black Sea region. The ca. 48 m thick Roxolany loess-palaeosol sequence was first studied by P. Gozhik with his research team (Putievoditel, 1976; Gozhik *et al.*, 1995), demonstrating its potential for palaeoenvironmental reconstruction on the basis of granulometric, mineralogical, palaeomagnetic, palaeontological (molluscs, mammal fauna) analyses as well as radiocarbon and Thermoluminescence (TL) dating. Within these first studies, the authors suggested that the Brunhes/Matuyama magnetic reversal (ca. 780 ka) is in the lower part of the profile. Later, Tsatskin *et al.* (1998) provided a detailed description, proposing a revised stratigraphic interpretation of the loess-palaeosol horizons and palaeomagnetic data, and their correlation with the marine oxygen isotope stages (MIS). The authors re-identified the Brunhes/Matuyama boundary in the middle part of the section in loess unit L₆ at ca. 35 m depth of the Roxolany loess-palaeosol complex, which now enabled a solid correlation with other loess profiles in Europe and China (e.g. Tsatskin *et al.*, 2001; Dodonov *et al.*, 2006; Gendler *et al.*, 2006; Faustov *et al.*, 2009).

Tsatskin *et al.* (1998) were the first to describe a macroscopic visible tephra (volcanic ash fall) layer, the so-called 'Roxolany Tephra', within the initially proposed L₃ loess unit (corresponding to MIS 12, i.e. the period from 450 to 400 ka; Sartori, 2000). Tephras, in general, are useful chronological and/or synchronisation markers in terrestrial and marine palaeoenvironmental archives, if correlated via glass geochemical fingerprinting with known and dated volcanic events (e.g. Lowe, 2011). Loess-palaeosol complexes in the Middle and Lower Danube Basin have proven the preservation of tephras in different stratigraphic positions, although their chemical compositions, and thus their precise ages, were often poorly constrained due to the strong alteration of volcanic glass shards under the prevailing humid to semi-humid temperate climate (e.g. Horváth, 2001; Panaiotu *et al.*, 2001; Fitzsimmons *et al.*, 2013; Veres *et al.*, 2013; Marković *et al.*, 2015). Fedorowicz *et al.* (2012) provided a first detailed description of the mineralogical components of the Roxolany Tephra and suggested a

possible genetic link with Carpathian volcanic activity. However, this assumption still lacked the geochemical and chronological evidence from proximal and other distal tephra deposits. Many years of comprehensive research focusing on Roxolany have brought up a number of new, partially contradictory data in the chronostratigraphic diagnosis of the upper three loess units (Fig. 2), and, implicitly, the timing of tephra deposition varied depending on such interpretations (Putivnyk, 2000; Gozhik *et al.*, 2007; Boguckyi *et al.* [eds], 2013; Gozhik, 2013). According to the latest data, the ‘Roxolany Tephra’ is embedded within the Bug loess (*bg*) from the upper Pleniglacial of the Weichselian glaciation (MIS 2) (Gozhik *et al.*, 2007) (Fig. 2). It is overlain by two palaeosol layers of an interphase or interstadial rank, the *Prychornomorsk* (*pc*) and the *Dofinivka* (*df*) units, that have recently been radiocarbon dated at ca. 23.0 cal ka BP and 34.0 cal ka BP, respectively (Fedorowicz *et al.*, 2012; Łanczont *et al.*, 2015; this study Fig. 2, Table 1). The palaeosol underlying the tephra-bearing *bg* loess, the *Vytachiv* (*vt*) unit, has been attributed to the middle Pleniglacial (MIS 3) and is AMS radiocarbon dated between ca. 21.3 and 25.6 cal ka BP (Fedorowicz *et al.*, 2012; Łanczont *et al.*, 2015; this study Fig. 2, Table 1). The *vt* unit developed on the *Uday* (*ud*) loess, which is correlated with MIS 4 (Fig. 2). Infrared optically-stimulated luminescence (IR-OSL) dates of loess samples from ca. 9 m below the tephra revealed an age of 33.1 ± 2.6 ka (Fedorowicz *et al.*, 2012; this study Table 3), supporting both the radiocarbon-based chronology and the stratigraphic scheme developed by Gozhik *et al.* (1995; 2007). Further attempts to directly date phenocrysts of the Roxolany Tephra, however, led to unrealistically old ages of 50 ± 3 Ma ($^{40}\text{Ar}/^{39}\text{Ar}$; Tsatskin *et al.*, 1998; Sartori, 2000) and 11.83-14.54 Ma (K/Ar on amphibole and biotite; Fedorowicz *et al.*, 2012).

In this study, we provide the first geochemical glass data of the ‘Roxolany Tephra’ and a solid correlation scheme with its dated volcanic source in order to (1) clarify the younger chronostratigraphy of the Roxolany loess-palaeosol complex, and (2) extend the tephrostratigraphic framework in south-eastern Europe with the principal aim of providing means for comparing various records on a wider scale.

2. Samples and methods

2.1 Roxolany sampling site

The Roxolany outcrop is situated on the eastern bank of the Dniester estuary, about 40 km southwest of Odessa and ca. 1.5 km northwest of the village of Roxolany (Ukrainian: Roksolany), SW Ukraine ($46^{\circ}10'N$, $30^{\circ}27'E$) (Fig. 1). The ca. 48 m thick loess-palaeosol complex crops out along the ‘Zayach’ya Balka’ gully, which is deeply incised into the

sedimentary mantle of the VII Dniester terrace containing the late Tertiary mammal complex (Chepalyga, 1967; Putivnyk, 2000; Gozhik *et al.*, 2007; Gozhik, 2013). A sample was taken from the 2-3 cm thick, white-greyish tephra layer that occurs in the third upper loess unit at ca. 9.5 m depth (Fig. 2).

2.2 Ciomadul proximal samples

Potential sources for the Roxolany Tephra encompass nearby Eastern Mediterranean volcanoes, e.g. the Aegean Arc (ca. 1100 km to the SSW), southern Italian volcanic provinces (ca. 1500 km to the SW), Anatolian volcanoes (ca. 900-1300 km to the SSE and SE), and the East Carpathians volcanic complexes (i.e. Ciomadul, ca. 350 km to the W) (Fig. 1). Late Quaternary tephrostratigraphies of Eastern Mediterranean volcanoes have been well constrained during the past decades (e.g. Keller *et al.*, 1978; Federman and Carey, 1980; Deniel *et al.*, 1998; Kuzucuoglu *et al.*, 1998; Druitt *et al.*, 1999; Narcisi and Vezzoli, 1999), while a detailed tephrostratigraphic framework of the East Carpathians is still in its infancy. Here, the Ciomadul volcanic massif in Romania, which is among the few candidates with Quaternary eruptions, is proposed to be the site of the youngest activity in the Carpatho-Pannonian Region. The timing of its activity is confined either to the past 1 Ma (Szakács *et al.*, 2015) or only to the past 250-200 ka (Karátson *et al.*, 2013; Harangi *et al.*, 2015) and requires further studies. The Ciomadul volcanic massif is located in the South Harghita Mountains at the southernmost tip of the 140 km-long Călimani-Gurghiu-Harghita (CGH) volcanic range, representing the south-eastern part of the Miocene to Pleistocene volcanic range of the East Carpathians (e.g. Seghedi *et al.*, 2004, Pécskay *et al.*, 2006). Compared to other parts of the calc-alkaline Neogene Carpathian volcanic region, complex, subduction-related, post-collisional volcanism occurred along the CGH (Mason *et al.*, 1998; Chalot-Prat and Gîrbacea, 2000; Seghedi *et al.*, 2004), which is characterised by an obvious along-arc migration from the northwest to the southeast since ca. 10 Ma (Pécskay *et al.*, 1995, 2006). The Ciomadul volcanic massif is a dome complex built on top of folded and thrustured Lower Cretaceous flysch sediments. Its central edifice (Ciomadul Mare, 1301m a.s.l.) is truncated by two explosion craters: the older Mohoş crater peat bog in the east and the younger St. Ana crater lake in the west (Fig. 1). The latest volcanism at the Ciomadul/South Harghita volcanic complex produced pyroclastic deposits and lavas of fairly homogeneous high-K dacitic bulk-rock composition with a typical enrichment in incompatible trace elements (e.g. Szakács and Seghedi 1986; Szakács *et al.*, 1993; Mason *et al.*, 1998), and a main mineral assemblage of plagioclase, amphibole, biotite, occasional clinopyroxene, quartz, K-feldspar, orthopyroxene

and olivine (e.g. Szakács and Seghedi, 1986; Mason *et al.*, 1998; Kiss *et al.*, 2014). However, in contrast to the bulk rock composition, the first volcanic glass chemical data obtained by Vinkler *et al.* (2007) on a pumiceous pyroclastic sequence near Băile Tuşnad indicate a more evolved (rhyolitic) composition of juvenile clasts.

A new and comprehensive tephrostratigraphic study has now been undertaken to characterize the glass compositions of numerous (>100) pyroclastic fall deposits from Ciomadul's latest activity in proximal and medial-distal settings around the volcanic complex and to provide solid chronostratigraphical constraints. The first results have revealed at least three eruptive stages from, probably, the Mohoş and St. Ana craters producing tephra of distinct rhyolitic glass compositions (Karátson *et al.*, 2016): The Early Phreatomagmatic and Plinian Activity (EPPA) at ≥ 51 ka - 43 cal ka BP, the Middle Plinian Activity (MPA) at ca. 31.5 cal ka BP and the Latest St. Ana Phreatomagmatic Activity (LSPA) at ca. 29.6 cal ka BP. Representative tephra from each eruptive stage have been chosen for this study to undertake a detailed geochemical comparison with the Roxolany Tephra (Fig. 5). Single-grain glass chemical data of these selected samples are published in Karátson *et al.* (2016) and are, additionally, presented here in the Supplementary Information. Representative samples include two pyroclastic fall units from an outcrop along community road no. 113, ca. 0.5 km W of Turia village and 11 km ESE of Lake St. Ana (hereafter referred to as "TUR-2" locality). This exposure at an abandoned gas pipeline reveals a basal, >1.5-m-thick stratified tuff and tuffaceous sand sequence (unit TUR-2.1) overlain by loess and loessy sands that are intercalated by a ca. 10-cm-thin pumiceous lapillistone bed (unit TUR-2.2) (Karátson *et al.*, 2016). On the basis of major element glass chemical data of pumices from both pyroclastic units it was possible to assign unit TUR-2.1 to the early phase of the EPPA stage (≥ 51 ka) and unit TUR-2.2 to the 'TGS' pumice fall eruption of the MPA stage at ca. 31.5 cal ka BP (Karátson *et al.*, 2016). Two further tephra layers were sampled from a lacustrine sediment sequence from the central part of the Mohoş crater (Fig 1). Core MOH-2 was retrieved by a UWITECH piston corer in 2014 and encompasses a ca. 30m-long sequence of Holocene peat (ca. 10 m) and last glacial lacustrine deposits that are intercalated with several dm-thick, coarse primary and reworked tephra layers. The two uppermost tephra layers at 1521.5-1544 cm and 1552-1564 cm depth, namely samples RO-1/2/3 and RO-4/5, are interpreted as primary fall layers that correspond to the LSPA (ca. 29.6 cal ka BP) and MPA eruptive stages (ca. 31.5 cal ka BP), respectively (Karátson *et al.*, 2016). Last but not least, we obtained geochemical glass data of coarse pumice fragments from the basal part of the St. Ana lake

core SZA-2013 from 1605-1612 cm depth. The SZA-2013 core retrieval also used a UWITECH piston corer and encompasses a total of 1700 cm of lacustrine sediments (Magyari *et al.*, 2014; Karátson *et al.*, 2016). The coarse pumice layers in the lowermost part of the sequence are interpreted as re-deposited pyroclastic material from the final (LSPA) eruption that formed the recent St. Ana crater, indicating that core SZA-2013 likely reached the bottom of the lacustrine deposits (Magyari *et al.*, 2014).

2.3 Radiocarbon dating

Radiocarbon (AMS) dating of the Roxolany Tephra's over- and underlying palaeosols of interphase or interstadial rank included ten organic soil samples, and was performed at the Poznan Radiocarbon Laboratory, Poland. All palaeosols represent dry steppe soils with A-B_k profiles and are affected by pedogenetic processes (i.e. rubification) of different degrees. Two samples were taken from the humus horizon of the palaeosol within the *pc* loess unit at 4.05 m (sample Roksolany 1) and 4.25 m depth (Roksolany 2). Three samples were collected from the underlying humus horizon of the upper *df1* palaeosol at 6.75 m (Roksolany 3) and 6.85 m depth (Roksolany 4, 4a), and two samples from the lower *df2* palaeosol at 7.05 m depth (Roksolany 5, 5a) (Table 1, Fig. 2). The humus horizon of the *vt* palaeosol (underlying the Roxolany Tephra) was sampled for radiocarbon dating at 20.2 m (Roksolany 6), 20.4 m (Roksolany 7) and 20.7 m depth (Roksolany 8). Radiocarbon dating results are published in Łanczont *et al.* (2015), but have been re-calibrated and presented as 2 σ ranges in Table 1.

AMS-¹⁴C dating of the MOH-2 core (Mohoš crater, Ciomadul) was carried out at the University of Cologne (CologneAMS), Germany, and encompassed three measurements on charcoal and bulk sediments above tephra RO-1/2/3 (two samples at 1369-1371 cm and 1519-1521.5 cm depth) and below tephra RO-4/5 (one sample at 1591-1593 cm depth), respectively (Table 2). All samples were pre-treated according to Rethemeyer *et al.* (2013), with the graphite targets measured by the accelerator mass spectrometry (AMS) at the University of Cologne.

Radiocarbon ages of the Roxolany and MOH-2 sequences were converted into calendar ages using the OxCal programme v4.2.2 (Bronk Ramsey 2008, 2009; Bronk Ramsey *et al.*, 2013) and the INTCAL13 calibration curve after Reimer *et al.* (2013), and are presented as calibrated age ranges with a confidence level of 95.4% in calendar years before present (cal yr BP).

2.4 IR-OSL dating

Dating of the Roxolany loess was performed by infrared optically stimulated luminescence (IR-OSL) dating at the Tallinn University of Technology, Estonia (Research Laboratory for Quaternary Geochronology). The luminescence dating method used potassium feldspar grains of the grain size range 100–150 μm . Palaeodose ' P ' (or equivalent dose ' D_e ') determinations were made by extrapolating the dose-response curves to zero IR-OSL intensities using the multiple-aliquot additive-dose protocol. Additive-dose growth curves were constructed using natural and ten-laboratory dose points each consisting of measurements of six separate aliquots. Aliquots of each sample were gamma-irradiated using a ^{60}Co source to a maximum dose of 1000 Gy. Preheating of the K-feldspar samples before the measurements was not applied. Instead, we stored samples for about 1 month at room temperature to allow the decay of post-irradiation phosphorescence (for details see Molodkov and Bitinas, 2006). Sediment matrix dose rates for the samples were calculated from the data of laboratory gamma-ray spectrometric analysis. Results of IR-OSL dating are displayed in Table 3.

2.5 Tephrochronological methods

Pumice samples from Ciomadul proximal sites were cleaned in deionized water, dried and crushed with a hammer into smaller grain sizes. The Roxolany Tephra was subsequently treated with a 15% hydrogen peroxide (H_2O_2) and a 10% hydrochloric acid (HCl) solution to remove organic remains and carbonates, respectively. Both Ciomadul and Roxolany tephtras were wet-sieved into a 32-125 μm grain size fraction. Dried tephra components were embedded on a slide with Araldit©2020 resin, sectioned by hand on silicon paper, polished and finally carbon coated for electron probe microanalyses (EPMA). The major element compositions of single glass shards were determined using a JEOL-JXA8230 instrument at the GFZ Potsdam using a 15 kV voltage, 10 nA beam current and beam sizes of 5-10 μm , respectively. Exposure times were 20 seconds for the elements Fe, Cl, Mn, Ti, Mg and P, as well as 10 seconds for Si, Al, K, Ca and Na. Instrumental calibration used natural minerals and the rhyolitic Lipari obsidian glass standard (Hunt and Hill, 1996; Kuehn *et al.*, 2011). Glass data are reported in Table 4 (Roxolany Tephra) and in the Supplementary Information (Ciomadul tephtras) and are compared in bivariate plots with published EPMA glass data of potential Eastern Mediterranean tephra correlatives (Figs. 4, 5).

Back-scattered electron (BSE) images of volcanic glass shards from different grain size fractions (32-63 μm , 63-125 μm and $>125 \mu\text{m}$) of the Roxolany Tephra were acquired with a

Hitachi TM3000 Tabletop Scanning Electron Microscope (SEM) at Keele University, U.K., using an accelerating voltage of 15 kV.

3. Results

3.1 Composition of the Roxolany tephra

The Roxolany Tephra is a fine-grained ($d_{\max} = 200 \mu\text{m}$) volcanic ash that is dominated by lithic clasts (dacitic rock fragments, clumped particles), phenocrysts (plagioclase, green pyroxene and biotite) and minor amounts of juvenile clasts (Figs. 3A-D). The latter consist of highly vesicular, microlite-rich (feldspars, pyroxenes) pumices (Fig. 3B) and blocky, low-vesicular glass shards (Figs. 3C, 3D), indicative of an origin from a phreatomagmatic eruption. Due to the mean low analytical totals of ca. 94-95 wt%, volcanic glasses are interpreted to be only slightly altered (Table 1). The major element glass composition is calc-alkaline rhyolitic with SiO_2 and Al_2O_3 concentrations of 75.6-77.6 wt% and 12.9-14.0 wt% (normalized, volatile-free data), respectively. Concentrations of FeO (0.5-0.9 wt%) and CaO (0.8-1.1 wt%) are low, and alkali ratios ($\text{K}_2\text{O}/\text{Na}_2\text{O}$) vary between 1.1 and 1.5 (Table 4, Figs. 4, 5).

3.2 Composition of Ciomadul proximal tephtras

The representative samples from Ciomadul's late stage activity reveal three distinct, partly overlapping major element glass compositions that indicate a clear compositional trend of matrix glass from highly evolved phreatomagmatic products (EPPA tephra) followed by the less evolved MPA/TGS pyroclastic units, and, finally, the slightly more evolved LSPA tephtras, the latter forming a group that falls compositionally in between the older eruption products (Karátson *et al.*, 2016) (Supplementary Information, Fig. 5). Pumice clasts of all three types are characterized by either a highly vesicular groundmass (MPA/TGS stage) and/or a larger number of microlite inclusions of feldspars, clinopyroxenes, amphiboles and Fe-Ti oxides (EPPA and LSPA stages). Therefore, a thorough evaluation of the major element glass data was required to avoid misinterpretations based on crystal contamination effects on groundmass glass composition. For this reason, beam sizes of EPMA were restricted to relatively small sizes that may have resulted in sodium migration during measurements (slightly higher SiO_2 and lower Al_2O_3 and Na_2O concentrations). However, the instrumental setup, including the beam sizes for EPMA of the Roxolany Tephra and potential Ciomadul correlatives were similar, and thus a reliable comparison of chemical glass data was achieved. In turn, attempts to obtain trace element glass data of both the Roxolany and Ciomadul

proximal tephra by larger-beam ($>10\ \mu\text{m}$) Laser Ablation (LA)-ICP-MS failed so far due to the high vesicularity and/or microlite content of juvenile clasts.

3.2.1 Sample TUR-2.1 (Early phreatomagmatic eruptions of EPPA stage, $\geq 51\ \text{ka}$)

Unit TUR-2.1 consists of low to medium vesicular pumice fragments that are characterised by a large amount of feldspar and Fe-oxide microlite inclusions. Matrix glass shows a heterogeneous, highly evolved rhyolitic composition, with ranges in concentrations (normalized volatile-free data) in SiO_2 of 76.4-79.7 wt%, Al_2O_3 of 11.5-13.4 wt%, FeO of 0.5-0.8 wt%, CaO of 0.6-1.1 wt% and $\text{K}_2\text{O}/\text{Na}_2\text{O}$ of 1.1-1.7 (Fig. 5).

3.2.2 Samples TUR-2.2 and RO-4/5 (Plinian eruption of MPA stage, ca. 31.5 cal ka BP)

Sample TUR-2.2 and tephra layer RO-4/5 in Mohoş core MOH-2, 15.52-15.64 m depth, comprise highly vesicular pumice fragments with a minor microlite assemblage. Volcanic glass of both samples revealed a similar rhyolitic composition that is less evolved than that of the older EPPA sample TUR-2.1. Major element concentrations show ranges in SiO_2 of 70.3-73.9 wt%, Al_2O_3 of 14.7-16.8 wt%, FeO of 0.9-1.6 wt%, CaO of 1.0-2.0 wt% and $\text{K}_2\text{O}/\text{Na}_2\text{O}$ of 0.7-1.2 (Fig. 5).

3.2.3 Samples RO-1/2/3 and SZA-2013, 1605-1612cm (LSPA phreatomagmatic eruption, ca. 29.6 cal ka BP)

The uppermost tephra RO-1/2/3 at 1521.5-1544 cm depth in Mohoş core MOH-2 is a coarse, reversely graded pumice fallout that was deposited in a lacustrine environment. Pumices are slightly blocky-angular, low to medium vesicular and rich in feldspar microlites. The major element glass composition shows a heterogeneous, intermediate rhyolitic composition that is slightly less evolved than that of EPPA-type tephra units with SiO_2 concentrations of 74.7-78.0 wt%, slightly higher Al_2O_3 (12.3-14.0 wt%), FeO (0.3-1.0 wt%) and CaO (0.6-1.1 wt%) values, as well as alkali ratios $\text{K}_2\text{O}/\text{Na}_2\text{O}$ of 1.1-1.6. This LSPA-type glass composition is comparable with that of the re-deposited pyroclastic layers from the basal part of the Lake St. Ana sediment core (sample SZA-2013 from 1605 to 1612 cm depth; Fig. 5).

4. Source and associated age of the Roxolany Tephra

The glass composition of the Roxolany Tephra was compared with EPMA glass data of other Late Pleistocene tephra occurring in the Eastern Mediterranean. Calc-alkaline rhyolitic

tephras were produced from several volcanic centres of the Aeolian (Italy) and Aegean Arcs (Greece), Anatolia (Turkey) and the East Carpathians (Romania) during the considered time span between ca. 50 and 20 ka (Fig. 1).

Lipari Island in southern Italy (ca. 1530 km SW of Roxolany), for example, erupted the Monte Guardia rhyolites between 27 and 24 cal ka BP (e.g. Forni *et al.*, 2013). However, this sub-plinian eruption had only limited regional tephra dispersal (e.g. Crisci *et al.*, 1991; Lucchi *et al.*, 2008; Forni *et al.*, 2013), and the respective juvenile pyroclasts show a distinct major-element composition with lower concentrations in SiO₂ and higher FeO concentrations compared to the Roxolany Tephra (Fig. 4).

The Lower and Upper Pumices from Nisyros (Aegean Arc, ca. 1100 km SSW of Roxolany) are dated at >50 ka (Margari *et al.*, 2007; Tomlinson *et al.*, 2012; Karkanis *et al.*, 2015) and show a similar glass composition to the Roxolany Tephra except for higher FeO and slightly lower Al₂O₃ values. Both Nisyros tephras have been found as discrete layers in marine sites south of the vent (Keller *et al.*, 1978), but were not identified in northern locations so far except for the Upper Pumice that was recently reported as a cryptotephra within the Theopetra cave where it is stratigraphically overlain by the Pantellerian Y6/Green Tuff, dated at 45.7 ka (Karkanis *et al.*, 2015). In the more proximal marine stratigraphy, the Upper Nisyros Pumice is overlain by the ca. 31 ka Yali-C (Yali-2) tephra (Federman and Carey, 1980), which in turn has a limited regional dispersal and a distinct rhyolitic composition compared to the Roxolany tephra (Fig. 4). The Y-2/Cape Riva tephra (22 cal ka BP) from Thera volcano (Santorini, Aegean Arc, ca. 1150 SSW of Roxolany) has been widely distributed towards the north (>500 km) and the northeast (>700 km) (e.g. Wulf *et al.*, 2002; Kwiecien *et al.*, 2008; Müller *et al.*, 2011). However, the glass chemical composition of the Y-2 tephra is less silicic rhyolitic (Fig. 4), and thus this tephra can be excluded as a potential correlative of the Roxolany Tephra.

Anatolian stratovolcanoes and caldera complexes, i.e. Acigöl and Erciyes Dağı (Central Anatolian Volcanic Province (CAVP), ca. 900-950 km SSE of Roxolany), and Süphan and Nemrut Dağı (East Anatolian Volcanic Province (EAVP), ca. 1280 km SE of Roxolany), produced numerous pyroclastic fallout deposits of highly silicic rhyolitic glass compositions during the considered time frame (e.g. Druitt *et al.*, 1995; Deniel *et al.*, 1998; Kuzucuoglu *et al.*, 1998; Sumita and Schmincke, 2013b) (Fig. 4). Especially the MIS2 tephras from Acigöl and Süphan Dağı come close to the major element composition of the Roxolany Tephra (Fig. 4). Those tephras, however, have so far only been recognized close to their volcanic centres (e.g. visible tephra layers from Süphan Dağı in Lake Van sediments; Sumita and Schmincke, 2013a; Schmincke *et al.*, 2014) and potentially as cryptotephra layers (macroscopic non-

visible tephra layers) in south-eastern Black Sea sediments (Cullen *et al.*, 2014) (Figs. 1 and 5). Other CAVP tephras that show compositions comparable to the Roxolany Tephra, e.g. early Holocene deposits from Erciyes Dađı, are dispersed towards the south (Develle *et al.*, 2009; Hamann *et al.*, 2010) and too young to be considered as correlatives.

The large thickness and maximum grain sizes of the Roxolany tephra, however, suggest a rather nearby source, e.g. the Ciomadul volcano in the southern East Carpathians located ca. 350 km W of the Roxolany site. Ciomadul's latest tephras are dispersed towards the N (e.g. EPPA-stage tephras), the S/SE (both EPPA- and MPA/TGS-stage tephras), and likely towards the E (LSPA-stage tephra) (Karátson *et al.*, 2016). Representative rhyolitic glass compositions of the older EPPA (≥ 51 ka) and MPA/TGS tephras (ca. 31.5 cal ka BP) are distinct from that of the Roxolany Tephra, with the oldest EPPA tephra (e.g. sample TUR-2.1) being the more evolved (mean high SiO₂ values of ca. 78 wt%) and the MPA/TGS tephra (e.g. samples TUR-2.2 and RO-4/5) the less silicic products (mean SiO₂ concentration of ca. 73 wt%) (Fig.5). Major-element glass data of the youngest, chemically intermediate LSPA tephra (mean SiO₂ values of 76.5 wt%), e.g. samples RO-1/2/3 and SZA-2013, 1605-1612 cm, in turn, match the glass data composition of the Roxolany Tephra and are here proposed as the correlative pyroclastic deposit (Fig. 5). The phreatomagmatic character, as inferred from low vesicularity pumice fragments, furthermore supports the geochemical evidence, as well as the large thickness and maximum grain sizes of the Roxolany Tephra, which imply a relatively short transport from the St. Ana crater by prevailing westerly winds. The LSPA tephra is dated at 29.6 ± 0.62 cal yr BP by radiocarbon age interpolation of tephra sample RO-1/2/3 in the MOH-2 core (Fig. 6A, Table 2). A second age approximation is given at $>27.18 \pm 0.46$ cal yr BP from ¹⁴C dates on pollen concentrates from the lowermost part of the St. Ana SZA-2013 sediment sequence, which can be considered as a minimum age of the onset of lake sedimentation after the final, crater-forming eruption (Karátson *et al.*, 2016).

5. Roxolany chronostratigraphy

The correlation of the Roxolany Tephra with the final eruptive products of Ciomadul volcano confirms the proposed time constraints of tephra-embedding sediments at Roxolany during the Last Glacial Maximum (Figs. 2, 6B). Therefore, the chronostratigraphy of the uppermost part of the Roxolany loess-palaeosol sequence is constrained by three different dating methods encompassing radiocarbon dating of palaeosols, IR-OSL loess dating and tephrochronology.

Radiocarbon dating of palaeosols in loess deposits is generally problematic, as the soil system remains open for a relatively long period (Orlova and Panychev, 1993). Thus, AMS- ^{14}C dating of the organic soil samples at Roxolany gave partly mixed ages, i.e. in the upper two palaeosols of interphase rank between ca. 23,000 and 34,000 cal yr BP, and partly reversed ages, i.e. in the lower *vt* pedocomplex between 21,350 and 25,600 cal yr BP (Łanczont *et al.*, 2015) (Table 1, Fig. 2). Mixed ages of the studied palaeosols can have a complex origin. They likely resulted from the low humus content of 0.13 to 0.18wt% (Łanczont *et al.*, 2015) but also from the specific features of loess, which was the parent material of these soils. Silt alluvia with a high admixture of organic matter were very likely the source material for loess. They were deposited by the Dniester River in the shelf area, which was widely exposed as a result of the Late Pleistocene sea regression, and consequently very intensively blown during the formation of *ud* and *bg* loess deposits (Gozhik, 2013). Reversed ages in the lower *vt* pedocomplex are also difficult to explain. Those samples were obtained from the bottom part of a wall at a deep ravine, which is strongly overgrown by shrubs, i.e. in the zone of penetration of roots and concentrated flow of rainwater. Thus, we cannot exclude contamination of the samples by modern organic material, which in turn resulted in younger radiocarbon dates. In order to construct a consistent deposition (age-depth) model using Bayesian statistics we only selected radiocarbon dates that were most likely not influenced by older carbon, i.e. samples Roksolany 1, 2, combined 4/4a and 5/5a from the two upper palaeosols (Table 1, Fig. 6B). Radiocarbon dates of the lower *vt* pedocomplex are interpreted as too young based on the IR-OSL date of the overlying *bg* loess of 33.1 ± 2.6 ka (Table 3) and thus have been rejected.

The imported Roxolany Tephra age of $29,589 \pm 620$ cal yr BP derives from linear interpolation of two Bayesian modelled AMS- ^{14}C dates at $27,832 \pm 652$ and ca. $29,575 \pm 618$ cal yr BP, ca. 151.5 cm and 1.25 cm (mean depths) above the RO-1/2/3 tephra, respectively, in the proximal MOH-2 core (Fig. 6A). It is chronostratigraphically in agreement with the age of the underlying MPA/TGS tephra (sample RO-4/5) at ca. $31,450 \pm 260$ cal yr BP (Harangi *et al.*, 2010; Karátson *et al.*, 2016) and a radiocarbon age of bulk sediments at $31,749 \pm 894$ cal yr BP ca. 27 cm below the RO-4/5 tephra.

The Roxolany Tephra age at ca. 29.6 cal ka BP obtained at Ciomadul volcano is consistent within the radiocarbon and IR-OSL age based age-depth model of the upper Roxolany sequence and thus can be integrated into the Bayesian age model (Fig. 6B). Accordingly, we can estimate a mean sedimentation rate of the Bug loess unit of ca. 2-3 mm/yr, pointing to

very high accumulation rates during the last glacial period that also favoured the preservation of tephra within the loess sequence.

6. Implication for the distal tephrostratigraphy of Ciomadul volcano

The identification of the LSPA tephra from Ciomadul volcano at the distal site of Roxolany has further implications on the tephrostratigraphic framework of the Eastern Mediterranean – Black Sea region, particularly for linking the widespread loess records, the detailed correlation which is still hampered by limited chronological control (Veres *et al.*, 2013; Markovic *et al.*, 2015). The finding of a 2-3 cm thick tephra layer indicates on the one hand an exceptional preservation in loess sediments, probably due to high sedimentation rates and related rapid covering of the tephra by wind-blown sediments (Chlebowski *et al.*, 2003; Boguckyi *et al.* [eds], 2013). This minimum thickness in combination with the relatively large grain size of tephra components at ca. 350 km distance suggests an origin from a violent, possibly even phreatoplinian eruption and widespread dispersal of the LSPA tephra by strong westerly winds. We thus expect further LSPA tephra and cryptotephra findings beyond the Roxolany site (e.g. in Eastern Romania, Ukraine and southern Russia) in the near future. Similarly, a wider dispersal of the older EPPA and MPA/TGS tephtras from Ciomadul in a southerly/south-easterly direction, i.e. at sites in southern Romania, the Balkans, Black Sea and beyond, can be anticipated. Sediment core M72/5-25-GC1 from the south-eastern Black Sea (Fig.1), located ca. 1050 km ESE of Ciomadul, has already been proposed as such a potential site of Ciomadul cryptotephra preservation, but no solid tephra correlation was possible so far (Cullen *et al.*, 2014). The comparison of new major-element glass chemical and chronostratigraphic data from Ciomadul's latest explosive activity with 48.3-25 ka cryptotephra data of the Black Sea core (BSC) allows as well only tentative correlations (Fig. 4). For instance, the less evolved glass population of cryptotephra BSC_651, dated between 25 ka and 34.4 ka (Nowaczyk *et al.*, 2012; Cullen *et al.*, 2014), has a strong affinity to the 31.5 ka MPA/TGS tephra except for the lower CaO concentrations (Fig. 4). Older cryptotephtras from the Black Sea core dated between 34.4 ka and 48.3 ka are geochemically indistinctive from each other and may correlate either with the older EPPA tephtras from Ciomadul or the EAPV (Süphan) tephtras (Figs. 3,4). In these cases, trace element and isotopic data sets of glass shards from all – proximal and distal – archives will be required for further detangling.

6. Summary and Conclusions

The tephrochronological study of the Roxolany loess site in combination with new geochemical and chronostratigraphic tephra constraints from the latest explosive activity of Ciomadul volcano (East Carpathians) allows a robust correlation of the long-discussed Roxolany Tephra with the final LSPA eruption of Ciomadul. The age of the LSPA tephra is constrained at the source volcano at ca. 29.6 cal ka BP and is in good agreement with the recently obtained dates for the Roxolany Tephra embedding sediments. Therefore, we propose that the Roxolany Tephra was deposited during the onset of the Last Glacial Maximum of the Weichselian phase, a period of intense aeolian activity. The occurrence of a visible Ciomadul tephra layer ca. 350 km east of its vent has important implications for future (crypto) tephra findings in the south-eastern Mediterranean and Black Sea region that would integrate Carpathian volcanism into establishing a regional tephra framework that focuses on linking terrestrial (loess and alluvial) and marine records.

Acknowledgements

This study was supported by the projects No. NN306 474138 and No. 691-N/2010/0 Ukraine of the Polish Ministry of Science and Higher Education. Furthermore, financial support by Hungarian National Funds K115472 and NF101362 was provided. D.V. acknowledges the support by a grant of the Ministry of National Education, CNCS–UEFISCDI, project number PN-II-ID-PCE-2012-4-0530. M.B. received funding from the German Research Council DFG, SFB 806 "Our Way to Europe". We are very grateful to Richard Niederreiter and his UWITEC team who performed the coring of both craters (St. Ana in 2013 and Mohoş in 2014). Coring was financially supported by the Hungarian National Fund NF101362 (St. Ana, 2013), and the German Science Foundation (DFG) as part of the CRC-806 "Our Way to Europe" at Cologne University, Germany (Mohoş, 2014), respectively. We also thank the ¹⁴C lab of Janet Rethemeyer (CologneAMS) for the radiocarbon dating of the MOH-2 sediment core samples. We extend our gratitude to the editor, Geoffrey Duller, and two anonymous referees for their constructive comments and suggestions on an earlier version of the manuscript.

References

Boguckiy A, Gozhik P, Lanczont M, Madeyska T, Jelovichowa J (eds). 2013. Loess cover in the north Black Sea area. *XVIII Polish-Ukrainian Seminar*. KARTPOL s.c. Lublin, 268 pp.

Bronk Ramsey C. 2008. Deposition models for chronological records. *Quaternary Science Reviews* **27** : 42-60.

Bronk Ramsey C. 2009. Bayesian analysis of radiocarbon dates. *Radiocarbon* **51** : 337-360.

Bronk Ramsey C, Scott EM, van der Plicht J. 2013. Calibration for archaeological and environmental terrestrial samples in the time range 26-50 ka cal BP. *Radiocarbon* **55** (4) : 20121-2027.

Çağatay MN, Wulf S, Ümmühan S, Özmaral A, Vidal L, Henry P, Appelt O, Gasperini L. 2015. The tephra record from the Sea of Marmara for the last ca. 70 ka and its palaeoceanographic implications. *Marine Geology* **361** : 96-110.

Chalot-Prat F, Gîrbacea R. 2000. Partial delamination of continental mantle lithosphere, uplift-related crust-mantle decoupling, volcanism and basin formation: a new model for the Pliocene-Quaternary evolution of the southern East-Carpathians, Romania. *Tectonophysics* **327** : 83-107.

Chepalyga AL. 1967. Antropogenovye presnovodnye molyuski Yuga Russkoi ravniny i ikh stratigraficheskoye znachenie [Quaternary fresh-water molluscs in the South of the Russian plain and their stratigraphic importance]. *Nauka*, Moscow, 222 pp.

Chlebowski R, Gozhik P, Lindner L, Lanczont M, Wojtanowicz J. 2003. Stratigraphy and sedimentology of the Bug loess (Pleistocene: Upper Vistulian) between Kiev and Odessa (Ukraine). *Geological Quarterly* **47** : 261-268.

Crisci GM, De Rosa R, Esperanca S, Mazzuoli R, Sonnino M. 1991. Temporal evolution of a three component system: the island of Lipari (Aeolian Arc, southern Italy). *Bulletin of Volcanology* **53** : 207-221.

Cullen VL, Smith VC, Arz HW. 2014. The detailed tephrostratigraphy of a core from the south-east Black sea spanning the last ~ 60 ka. *Journal of Quaternary Science* **29** : 675-690.

Deniel C, Aydar E, Gourgau A. 1998. The Hasan Dagi stratovolcano (Central Anatolia, Turkey): evolution from calc-alkaline to alkaline magmatism in a collision zone. *Journal of volcanology and Geothermal Research* **87** : 275-302.

Develle A-L, Williamson D, Gasse F, Walter-Simonnet A-V. 2009. Early Holocene volcanic ash fallout in the Yammoûneh lacustrine basin (Lebanon): Tephrochronological implications for the Near East. *Journal of Volcanology and Geothermal Research* **186** : 416-425.

Dodonov AE, Zhou LP, Markova AK, Tchepalyga AL, Trubikhin VM, Aleksandrovski AL, Simakova AN. 2006. Middle – Upper Pleistocene bio-climatic and magnetic records of the Northern Black Sea Coastal Area. *Quaternary International* **149** : 44–54.

Druitt TH, Brenchley PJ, Gökten YE, Francaviglia V. 1995. Late Quaternary rhyolitic eruptions from the Acigöl Complex, central Turkey. *Journal of the Geological Society, London* **152** : 655-667.

Druitt TH, Edwards L, Mellors RM, Pyle DM, Sparks RSJ, Lanphere M, Davies M, Barreiro B. 1999. Santorini Volcano. *Geological Society, London, Memoirs*, **19**.

- Faustov SS, Virina EI, Tsatskin A, Gendler TS, Heller F. 2009. The Matuyama/Brunhes boundary in loess sections in the south of the East European Plain and their correlation on the basis of palaeomagnetic and palaeopedologic data. *Quaternary International* **201** : 60-66.
- Federman AN, Carey SN. 1980. Electron microprobe correlation of tephra layers from Eastern Mediterranean abyssal sediments and the island of Santorini. *Quaternary Research* **13** : 160 - 171.
- Fedorowicz S, Wozniak PP, Halas S, Lanczont M, Paszkowski M, Wójtowicz A. 2012. Challenging K-Ar dating of the Quaternary tephra from Roxolany, Ukraine. *Mineralogia - Special Papers* **39** : 102-105.
- Fitzsimmons K, Hambach U, Veres D, Iovita R. 2013. The Campanian Ignimbrite eruption: new data on volcanic ash dispersal and its potential impact on human evolution. *PLoS One* **8/6**: e65839. <http://dx.doi.org/10.1371/journal.pone.0065839>
- Forni F, Lucchi F, Peccerillo A, Tranne CA, Rossi PL, Frezzotti ML. 2013. Stratigraphy and geological evolution of the Lipari volcanic complex (central Aeolian archipelago). *Geological Society, London, Memoirs* **37** : 213-279.
- Gendler TS, Heller F, Tsatskin A, Spassov S, Du Pasquier J, Faustov SS. 2006. Roxolany and Novaya Etuliya - key sections in the western Black Sea loess area: Magnetostratigraphy, rock magnetism, and paleopedology. *Quaternary International* **152-153** : 78-93.
- Gozhik P. 2013. Do pytannya vyvchennya pozrizu Roksolany. In: Boguckiy A. et al. (eds). 2013. Loess cover in the north Black Sea area. *XVIII Polish-Ukrainian Seminar*. KARTPOL s.c. Lublin : 17-33.
- Gozhik P, Komar M, Krohmal O, Shelkopyas V, Khrystoforova T, Dykan N, Prylypko S. 2007. The key section of Neopleistocene subaerial deposits near Roxolany village (Odessa region). *Problemy serednoplejstocenogo interglacialu*. Lviv, Vid. Centr. LNU im. I. Franka, pp. 109-128.
- Gozhik P, Shelkopyas V, Khristoforova T. 1995. Development stages of loessial and facial formation in Ukraine (Stratigraphy of loess in Ukraine). Lublin. *Annales Universitatis Mariae Curie-Sclodowska*. Sec. B. **50** : 65-74.
- Hamann Y, Wulf S, Ersoy O, Ehrmann W, Aydar E, Schmiedl G. 2010. First evidence of a distal early Holocene ash layer in Eastern Mediterranean deep-sea sediments derived from the Anatolian volcanic province. *Quaternary Research* **73** : 497-506.
- Harangi S, Lukács R, Schmitt AK, Dunkl I, Molnár K, Kiss B, Seghedi I, Novothny Á, Molnár M. 2015. Constraints on the timing of Quaternary volcanism and duration of magma residence at Ciomadul volcano, east-central Europe, from combined U-Th/He and U-Th zircon geochronology. *Journal of Volcanology and Geothermal Research* **301** : 66-80.
- Harangi S, Molnár M, Vinkler AP, Kiss B, Jull AJT, Leonard AE. 2010. Radiocarbon dating of the last volcanic eruptions of Ciomadul volcano, Southeast Carpathians, eastern-central Euro. *Radiocarbon* **52** : 1498-1507.
- Horváth E. 2001. Marker horizons in the loesses of the Carpathian Basin. *Quaternary International* **76** : 157-163.

Hunt JB, Hill PG. 1996. An inter-laboratory comparison of the electron probe microanalysis of glass geochemistry. *Quaternary International* **34-36** : 229-241.

Karátson D, Telbisz T, Harangi S, Magyar E, Dunkl I, Kiss B, Jánosi C, Veres D, Braun M, Fodor E, Biró T, Kósik S, von Eynatten H, Lin D. 2013. Morphometrical and geochronological constraints on the youngest eruptive activity in East-Central Europe at the Ciomadul (Csomád) lava dome complex, East Carpathians. *Journal of Volcanology and Geothermal Research* **255** : 43-56.

Karátson D, Wulf S, Veres D, Magyar EK, Gertisser R, Timar-Gabor A, Novothny Á, Telbisz T, Szalai Z, Anechitei-Deacu V, Appelt O, Bormann M, Jánosi C, Hubay K, Schäbitz F. 2016. The latest explosive eruptions of Ciomadul (Csomád) volcano, East Carpathians - a tephrostratigraphic approach for the 52-29 ka BP time interval. *Journal of Volcanology and Geothermal Research* **319** : 29-51.

Karkanis P, White D, Lane CS, Stringer C, Davies W, Cullen VL, Smith VC, Ntinou M, Tsartsidou G, Kyparissi-Apostolika N. 2015. Tephra correlations and climatic events between the MIS6/5 transition and the beginning of MIS3 in Theopetra Cave, central Greece. *Quaternary Science Reviews* **188** : 170-181.

Keller J, Ryan WBF, Ninkovich D, Altherr R. 1978. Explosive volcanic activity in the Mediterranean over the past 200,000 yr as recorded in deep-sea sediments. *Geological Society of America Bulletin* **89** : 591 - 604.

Kiss B, Harangi S, Ntaflou T, Mason PRD, Pál-Molnár E. 2014. Amphibole perspective to unravel pre-eruptive processes and conditions in volcanic plumbing systems beneath intermediate arc volcanoes: a case study from Ciomadul volcano (SE Carpathians). *Contributions to Mineralogy and Petrology* **167** : 986.

Kuehn SC, Froese DG, Shane PAR, INTAV Intercomparison Participants. 2011. The INTAV intercomparison of electron-beam microanalysis of glass by tephrochronology laboratories: Results and recommendations. *Quaternary International* **246** : 19-47.

Kuzucuoglu C, Pastre J-F, Black S, Ercan T, Fontugne M, Guillou H, Hatté C, Karabiyikoglu M, Orth P, Türkecan A. 1998. Identification and dating of tephra layers from Quaternary sedimentary sequences of Inner Anatolia, Turkey. *Journal of Volcanology and Geothermal Research* **85** : 153-172.

Kwiecien O, Arz HW, Lamy F, Wulf S, Bahr A, Röhl U, Haug GH. 2008. Estimated reservoir ages of the Black Sea since the Last Glacial. *Radiocarbon* **50** : 1-20.

Łanczont M, Madeyska T, Bogucki A, Mroczek P, Hołub B, Łacka B, Fedorowicz S, Nawrocki J, Frankowski Z, Standzikowski K. 2015. Abiotic environment of the Palaeolithic oecumene in the peri- and meta-Carpathian zone [In:] M. Łanczont, T. Madeyska (eds) Palaeolithic oecumene in the peri- and meta-Carpathian zone, Wydawnictwo UMCS, Lublin: 55–457 (in Polish).

Lowe DJ. 2011. Tephrochronology and its application: A review. *Quaternary Geochronology* **6** : 107-153.

Lucchi F, Tranne CA, De Astis G, Keller J, Losito R, Morche W. 2008. Stratigraphy and significance of Brown Tuffs on the Aeolian Islands (southern Italy). *Journal of Volcanology and Geothermal Research* **177** : 49-70.

- Magyari EK, Veres D, Wennrich V, Wagner B, Braun M, Jakab G, Karátson D, Pál Z, Ferenczy G, St-Onge G, Rethemeyer J, Francois JP, von Reumont F, Schäbitz F. 2014. Vegetation and environmental responses to climate forcing during the Last Glacial Maximum and deglaciation in the East Carpathians: attenuated response to maximum cooling and increased biomass burning. *Quaternary Science Reviews* **106** : 278-298.
- Margari V, Pyle DM, Bryant C, Gibbard PL. 2007. Mediterranean tephra stratigraphy revisited: Results from a long terrestrial sequence on Lesvos Island, Greece. *Journal of Volcanology and Geothermal Research* **163** : 34-54.
- Marković SB, Stevens T, Kukla GJ, Hambach U, Fitzsimmons KE, Gibbard P, Buggle B, Zech M, Guo Z, Hao Q, Wu H, O'Hara Dhand K, Smalley IJ, Újvári G, Sümegei P, Timar-Gabor A, Veres D, Sirocko F, Vasiljević DA, Jary Z, Svensson A, Jović V, Lehmkuhl F, Kovács J, Svirčev Z. 2015. Danube loess stratigraphy — Towards a pan-European loess stratigraphic model. *Earth-Science Reviews* **148** : 228-258.
- Mason PRD, Seghedi I, Szakács A, Downes H. 1998. Magmatic constraints on geodynamic models of subduction in the Eastern Carpathians, Romania. *Tectonophysics* **297** : 157–176.
- Molodkov A, Bitinas A. 2006. Sedimentary record and luminescence chronology of the Lateglacial and Holocene aeolian sediments in Lithuania. *Boreas* **35** (2) : 244–254.
- Müller UC, Pross J, Tzedakis PC, Gamble C, Kotthoff U, Schmiedl G, Wulf S, Christanis K. 2011. The role of climate in the spread of modern humans into Europe. *Quaternary Science Reviews* **30** : 273-279.
- Narcisi B, Vezzoli L. 1999. Quaternary stratigraphy of distal tephra layers in the Mediterranean - an overview. *Global and Planetary Change* **21** : 31-50.
- Nowaczyk NR, Arz HW, Frank U, Kind J, Plessen B. 2012. Dynamics of the Laschamp geomagnetic excursion from Black Sea sediments. *Earth and Planetary Science Letters* **351-352** : 54-69.
- Orlova LA, Panychev VA. 1993. The Reliability of Radiocarbon Dating Buried Soils. *Radiocarbon* **35** : 369.
- Panaiotu CG, Panaiotu EC, Grama A, Necula C. 2001. Paleoclimatic record from a loess-paleosol profile in southeastern Romania. *Physics and Chemistry of the Earth, Part A: Solid Earth and Geodesy* **26(11)** : 893-898.
- Pécskay Z, Lexa J, Szakács A, Balogh K, Seghedi I, Konecny V, Kovács M, Márton E, Kaliciak M, Széky-Fux V, Póka T, Gyarmati P, Edelstein O, Rosu E, Žec B. 1995. Space and time distribution of Neogene-Quaternary volcanism in the Carpatho-Pannonian Region. *Acta Vulcanologica* **7** (2) : 15–28.
- Pécskay Z, Lexa J, Szakács A, Seghedi I, Balogh K, Konečný V, Zelenka T, Kovacs M, Póka T, Fülöp A, Márton E, Panaiotu C, Cvetković V. 2006. Geochronology of Neogene-Quaternary magmatism in the Carpathian arc and intra-Carpathian area: a review. *Geologica Carpathica* **57** : 511–530.
- Putievoditel X. 1976. VIII mezhdunarodnogo symozyuma po lessovym porodam Kiev-Odessa. Guidebook, Naukova dumka, 46 pp.

Putivnyk X. 2000. X polsko-ukrainskogo seminaru Korelaciya lesiv i lodovikovykh vidkladiv Polshi i Ukrainy. Guidebook, *ING NAN Ukrainy*, Kiev, 36 pp.

Reimer PJ, Bard E, Bayliss A, Beck JW, Blackwell PG, Bronk Ramsey C, Buck CE, Cheng H, Edwards RL, Friedrich M, Grootes PM, Guilderson TP, Haflidason H, Hajdas I, Hatté C, Heaton TJ, Hogg AG, Hughen KA, Kaiser KF, Kromer B, Manning SW, Niu M, Reimer RW, Richards DA, Scott EM, Southon JR, Turney CSM, van der Plicht J. 2013. IntCal13 and MARINE13 radiocarbon age calibration curves 0-50000 years calBP. *Radiocarbon* **55** (4) : 1869–1887.

Rethemeyer J, Fülöp R-H, Höfle S, Wacker L, Heinze S, Hajdas I, Patt U, König S, Stapper B, Dewald A. 2013. Status report on sample preparation facilities for ¹⁴C analysis at the new Cologne AMS center. *Nuclear Instruments and Methods in Physics Research Section B, Beam Interactions with Materials and Atoms* **294** : 168–172.

Sartori M. 2000. The Quaternary climate in loess sediments: Evidence from rock and mineral magnetic and geochemical analysis. PhD Thesis, Swiss Federal Institute of Technology, Zurich, Switzerland, 231 pp.

Schmincke H-U, Sumita M, Paleovan scientific team. 2014. Impact of volcanism on the evolution of Lake Van (eastern Anatolia) III: Periodic (Nemrut) vs. episodic (Süphan) explosive eruptions and climate forcing reflected in a tephra gap between ca. 14 ka and ca. 30 ka. *Journal of Volcanology and Geothermal Research* **285** : 195-213.

Seghedi I, Downes H, Szakács A, Mason PRD, Thirlwall MF, Rosu E, Pécskay Z, Márton E, Panaiotu C. 2004. Neogene/Quaternary magmatism and geodynamics in the Carpathian-Pannonian region: a synthesis. *Lithos* **72** : 117-146.

Sumita M, Schmincke H-U. 2013a. Impact of volcanism on the evolution of Lake Van I: evolution of explosive volcanism of Nemrut Volcano (eastern Anatolia) during the past >400,000 years. *Bulletin of Volcanology* **75** : 714.

Sumita M, Schmincke H-U. 2013b. Impact of volcanism on the evolution of Lake Van II: Temporal evolution of explosive volcanism of Nemrut Volcano (eastern Anatolia) during the past ca. 0.4 Ma. *Journal of Volcanology and Geothermal Research* **253** : 15-34.

Szakács A, Seghedi I. 1986. Chemical diagnosis of the volcanics from the southernmost part of the Harghita Mountains—proposal for a new nomenclature. *Rev. Roum. Geol. Geophys. Geogr., ser. Geologie* **30** : 41–48.

Szakács A, Seghedi I, Pécskay Z. 1993. Peculiarities of South Harghita Mts. as the terminal segment of the Carpathian Neogene to Quaternary volcanic chain. *Rev. Roum. Geol. Geophys. Geogr., ser. Geologie* **37** : 21– 36.

Szakács A, Seghedi I, Pécskay Z, Mirea V. 2015. Eruptive history of a low frequency and low-output rate Pleistocene volcano, Ciomadul, South Harghita Mts., Romania. *Bulletin of Volcanology* **77** : 12. <http://dx.doi.org/10.1007/s00445-014-0894-7>.

Tomlinson EL, Kinvig HS, Smith VC, Blundy JD, Gottsmann J, Müller W, Menzies MA. 2012. The Upper and Lower Nisyros Pumices: Revisions to the Mediterranean tephrostratigraphic record based on micron-beam glass geochemistry. *Journal of Volcanology and Geothermal Research* **243-244** : 69-80.

Tomlinson EL, Smith VC, Albert PG, Aydar E, Civetta L, Cioni R, Cubukcu E, Gertisser R, Isaia R, Menzies MA, Orsi G, Rosi M, Zanchetta G. 2015. The major and trace element glass compositions of the productive Mediterranean volcanic sources: tools for correlating distal tephra layers in and around Europe. *Quaternary Science Reviews* **118** : 48-66.

Tsatskin A, Heller F, Gendler TS, Virina EI, Spassov S, Du Pasquier J, Hus J, Hailwood EA, Bagin VI, Faustov SS. 2001. A new scheme of terrestrial paleoclimate evolution during the last 1.5 Ma in the western Black Sea region: integration of soil studies and loess magmatism. *Physics and Chemistry of the Earth* **26** : 911-916.

Tsatskin A, Heller F, Hailwood EA, Gendler TS, Hus J, Montgomery P, Sartori M, Virina EI. 1998. Pedosedimentary division, rock magnetism and chronology of the loess/palaeosol sequence at Roxolany (Ukraine). *Palaeogeography, Palaeoclimatology, Palaeoecology* **143** : 111-133.

Veres D, Lane CS, Timar-Gabor A, Hambach U, Constantin D, Szakacs A, Fülling A, Onac BP. 2013. The Campanian Ignimbrite/Y5 tephra layer: A regional stratigraphic marker for Isotope Stage 3 deposits in the Lower Danube region, Romania. *Quaternary International* **293** : 22-33.

Vinci A. 1985. Distribution and chemical composition of tephra layers from Eastern Mediterranean abyssal sediments. *Marine Geology* **64** : 143-155.

Vinkler AP, Harangi S, Ntaflou T, Szakács A. 2007. A Csomád vulkán (Keleti-Kárpátok) horzsaköveinek közettani és geokémiai vizsgálata - petrogenetikai következtetések (petrology and geochemistry of pumices from the Ciomadul volcano (Eastern Carpathians) - implications for petrogenetic processes). *Földt. Közl. (Bulletin of the Hungarian Geological Society)* **137** : 103-128.

Wulf S, Kraml M, Kuhn T, Schwarz M, Inthorn M, Keller J, Kuscu I, Halbach P. 2002. Marine tephra from the Cape Riva eruption (22 ka) of Santorini in the Sea of Marmara. *Marine Geology* **183** : 131-141.

Figure captions

Figure 1: (A) Landsat image (Google Earth 2015) of the central and eastern Mediterranean showing the location of main silicic volcanic centres and sites mentioned in the text. (B) Landsat image of the Ciomadul volcanic complex with St. Ana and Mohoš crater drilling sites and TUR-2 sampling location. (C) Schematic map of the Roxolany sampling site (red arrow).

Figure 2: Stratigraphy, lithology and dating results for the upper loess section at Roxolany. (A) General overview of the top loess-soil section with position of the volcanic ash layer. Radiocarbon age ranges of palaeosols include a 2σ error and used the OxCal program v4.2.4

after Bronk Ramsey (2008, 2009) and Bronk Ramsey *et al.* (2013) in combination with the INTCAL13 calibration curve (Reimer *et al.*, 2013). Original radiocarbon data from Łanczont *et al.* (2015). **(B)** MIS2 sediments at the Roxolany site, showing the Dofinivka soils (red-brownish top layer) and upper section of the Bug loess unit that contains the 2-3 cm thick white-greyish Roxolany tephra.

Figure 3: Backscattered electron (BSE) images of Roxolany Tephra components. (A) Overview of the 63-125 μm grain size fraction, (B) highly vesicular, microlite-rich pumiceous ash of the >125 μm fraction, (C) low-vesicular, microlite-rich glass shards with (D) attached feldspar micro-phenocryst of the 63-125 μm fraction. gl = volcanic glass; fs = feldspar; lt = lithic clast (clumped particles).

Figure 4: Geochemical bivariate plots of glass data of the Roxolany tephra in comparison with published data of potential eastern Mediterranean tephra sources. EPMA data are obtained from: Roxolany tephra (red stars): this study; Lipari: Crisci *et al.* (1991); Cape Riva/Y-2, Santorini: Çağatay *et al.* (2015), Tomlinson *et al.* (2015), Wulf *et al.* (2002); Yali-C: Federman and Carey (1980), Vinci (1985); Nisyros Lower and Upper Pumices: Tomlinson *et al.* (2012); Erciyes Dag and Acigöl: Tomlinson *et al.* (2015); Süphan Dagi and Nemrut Dagi: Schmincke *et al.* (2014).

Figure 5: Geochemical bivariate plots of glass data for discriminating between the Roxolany tephra (red stars, this study), proximal tephra deposits from the latest activity of Ciomadul volcano (black envelope = EPPA stage, orange envelope = MPA stage including TGS eruption, blue envelope = LSPA stage; after Karátson *et al.*, 2016), representative Ciomadul pumice samples (black, orange and blue symbols; this study and Karátson *et al.*, 2016) and cryptotephra of the last glacial period from Black Sea Core (BSC) M72/5-25-GC1 (grey fields; data from Cullen *et al.*, 2014).

Figure 6: Deposition models of (A) Mohoş MOH-2 core (1350-1600 cm depth, with core photographs) and (B) the upper Roxolany sequence (4-21m, with schematic lithological profile, for legend see Fig. 2) using the OxCal program v4.2.4 after Bronk Ramsey (2008, 2009) and Bronk Ramsey *et al.* (2013) in combination with the INTCAL13 calibration curve (Reimer *et al.*, 2013).

Table captions

Table 1: Results of radiocarbon AMS dating of palaeosols (bulk sediment) of the Roxolany site after Łanczont *et al.* (2015). Calibration used the OxCal software v4.2.4 (Bronk Ramsey 2008, 2009; Bronk Ramsey *et al.*, 2013) with the INTCAL13 calibration curve of Reimer *et al.* (2013). # Radiometric date not used for the Bayesian deposition model (see Fig. 6B).

Table 2: Results of radiocarbon AMS dating of sediments of the MOH-2 core from the Mohoş crater, Ciomadul, partly modified from Karátson *et al.* (2016). Calibration used the OxCal software v4.2.4 (Bronk Ramsey 2008, 2009; Bronk Ramsey *et al.*, 2013) with the INTCAL13 calibration curve of Reimer *et al.* (2013). *Mean radiocarbon age obtained from two charcoal samples from the Bixad outcrop south of Lake St. Ana, Ciomadul volcano (Harangi *et al.*, 2010; Vinkler *et al.*, 2007).

Table 3: IR-OSL results and radioactivity data of the loess sample from 18.7 m depth (Bug loess) of the Roxolany sequence.

Table 4: EPMA raw data of single point glass analyses of the Roxolany tephra and results of the rhyolitic Lipari Obsidian glass standard.

Table 1:

AMS ID	Sample ID	Depth (m)	Sample material	Comments	¹⁴ C age (yr BP)	Calibrated age range (cal yr BP), 2σ error
Poz-42403	Roksolany 1	4.05	humus horizon of the	TOC, 0.53mgC	19,510 ± 190	23,975 – 23,005
Poz-42404	Roksolany 2	4.25	palaeosol within the <i>pc</i> loess unit	TOC, 0.64mgC	19,920 ± 180	24,404 – 23,532
Poz-42405	Roksolany 3	6.75	humus horizon of the	TOC, 0.41mgC	25,890 ± 490	30,990 – 29,050 #
Poz-42406	Roksolany 4	6.85	<i>df1</i> palaeosol	TOC, 0.54mgC	24,140 ± 310	28,789 – 27,682
Poz-42407	Roksolany 4a	6.85		TOC, 0.77mgC	21,880 ± 200	26,590 – 25,770
Poz-42414	Roksolany 5	7.05	humus horizon of the	TOC, 0.48mgC	29,030 ± 430	34,002 – 31,914
Poz-42408	Roksolany 5a	7.05	<i>df2</i> palaeosol	TOC, 0.48mgC	20,180 ± 200	24,914 – 23,787
Poz-42415	Roksolany 6	20.2	humus horizon of the	TOC	18,410 ± 90	22,479 – 21,985 #
Poz-42417	Roksolany 7	20.4	<i>vt</i> palaeosol	TOC, 0.52mgC	17,970 ± 150	22,221 – 21,356 #
Poz-42418	Roksolany 8	20.7		TOC, 0.48mgC	20,820 ± 210	25,606 – 24,492 #

Table 2:

AMS ID	Sample ID	Composite depth (cm)	Sample material	C (µg)	¹⁴ C age (yr BP)	Calibrated age range (cal yr BP), 2σ error	Bayesian modeled age range (cal yr BP), 95.4% probability
COL3252.1.1	MOH-2.5-1369-1371	1369-1371	charcoal	139	23,529 ± 348	28,417 – 27,171	28,483 – 27,180
COL3253.1.1	MOH-2.7-1519-1521.5	1519-1521.5	sediment/soil	396	25,438 ± 207	30,221 – 28,996	30,192 – 28,957
	<i>LSPA-Tephra</i>	<i>1521.5-1544</i>	<i>Tephra RO-1/2/3</i>				<i>30,209 – 28,969</i>
	<i>MPA-Tephra</i>	<i>1552-1564</i>	<i>Tephra RO-4/5</i>			<i>31,710 – 31,190 *</i>	
COL3255.1.1	MOH-2.9-1591-1593	1591-1593	sediment/soil	587	27,533 ± 438	32,643 – 30,855	

Table 3:

Lab No.	Field No.	Site	U (ppm)	Th (ppm)	K (%)	Equivalent dose, d_e (Gy)	Dose rate, d_r (mGy/a)	Age (ka)
RLQG 2153-043	R-15	Roxolany	2.44 ± 0.01	8.57 ± 0.43	1.44 ± 0.03	111.3 ± 5.14	3.36 ± 0.17	33.1 ± 2.6

Table 4

Sample		SiO ₂	TiO ₂	Al ₂ O ₃	FeO _t	MnO	MgO	CaO	Na ₂ O	K ₂ O	P ₂ O ₅	Total	-Cl-
Roxolany	#1	73.35	0.06	12.33	0.54	0.05	0.03	0.89	3.17	4.41	0.03	94.86	0.14
	#2	72.44	0.09	12.49	0.58	0.06	0.03	0.71	3.33	4.85	0.00	94.58	0.17
	#3	71.94	0.09	12.54	0.74	0.03	0.06	0.92	3.54	4.52	0.03	94.41	0.18
	#4	71.97	0.05	12.03	0.67	0.06	0.05	0.89	3.26	4.13	0.00	93.11	0.17
	#5	72.97	0.07	12.25	0.59	0.02	0.04	0.86	3.34	4.44	0.02	94.60	0.21
	#6	71.78	0.07	12.22	0.45	0.06	0.01	0.97	3.49	3.78	0.03	92.86	0.16
	#7	73.62	0.10	12.21	0.60	0.01	0.03	0.77	3.76	3.82	0.00	94.92	0.18
	#8	72.46	0.10	12.80	0.83	0.02	0.01	0.86	3.75	4.62	0.00	95.45	0.26
	#9	72.33	0.04	12.12	0.49	0.05	0.01	0.92	2.99	4.51	0.07	93.53	0.17
	#10	72.58	0.10	12.43	0.68	0.08	0.04	0.88	3.40	4.44	0.00	94.63	0.21
	#11	73.10	0.07	12.30	0.50	0.04	0.02	0.93	3.34	4.41	0.00	94.71	0.17
	#12	72.81	0.06	12.32	0.54	0.02	0.02	0.93	3.37	4.14	0.00	94.21	0.19
	#13	72.83	0.05	12.35	0.54	0.07	0.05	0.86	3.02	4.63	0.00	94.40	0.17
	#14	71.07	0.08	12.28	0.63	0.05	0.05	0.89	3.30	4.19	0.01	92.55	0.19
	#15	71.77	0.12	12.57	0.64	0.01	0.05	0.89	3.59	4.58	0.04	94.26	0.17
	#16	71.25	0.09	12.62	0.72	0.05	0.04	0.91	3.53	4.51	0.00	93.72	0.19
<i>Lipari Obsidian</i>													
	10 μm-beam	73.61	0.09	12.87	1.55	0.06	0.03	0.71	4.02	5.22	0.02	98.18	0.37
	15 μm-beam	73.53	0.10	12.85	1.61	0.11	0.02	0.72	4.06	5.30	0.00	98.30	0.37
	20 μm-beam	73.56	0.05	12.78	1.49	0.11	0.05	0.72	4.01	5.26	0.00	98.03	0.34
Hunt and Hill (1996),	12 μm-beam	74.35	<i>n.a.</i>	12.87	1.51	0.07	0.05	0.74	3.93	5.11	<i>n.a.</i>	98.98	0.35

Figure 1



Figure 2

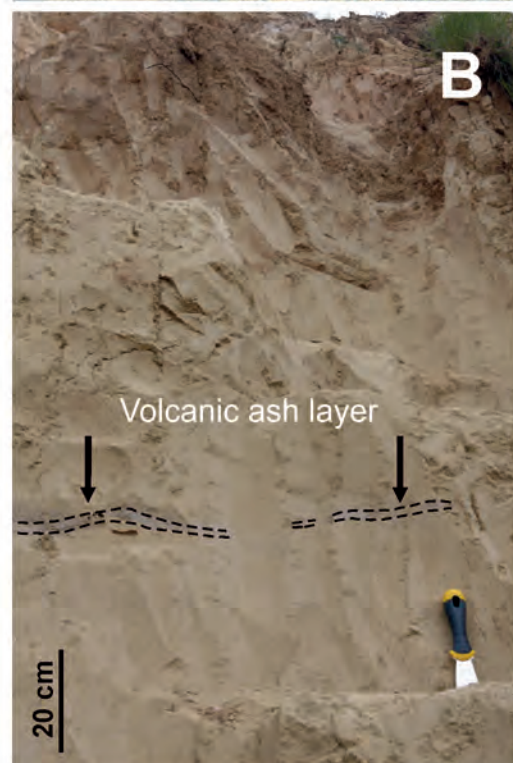
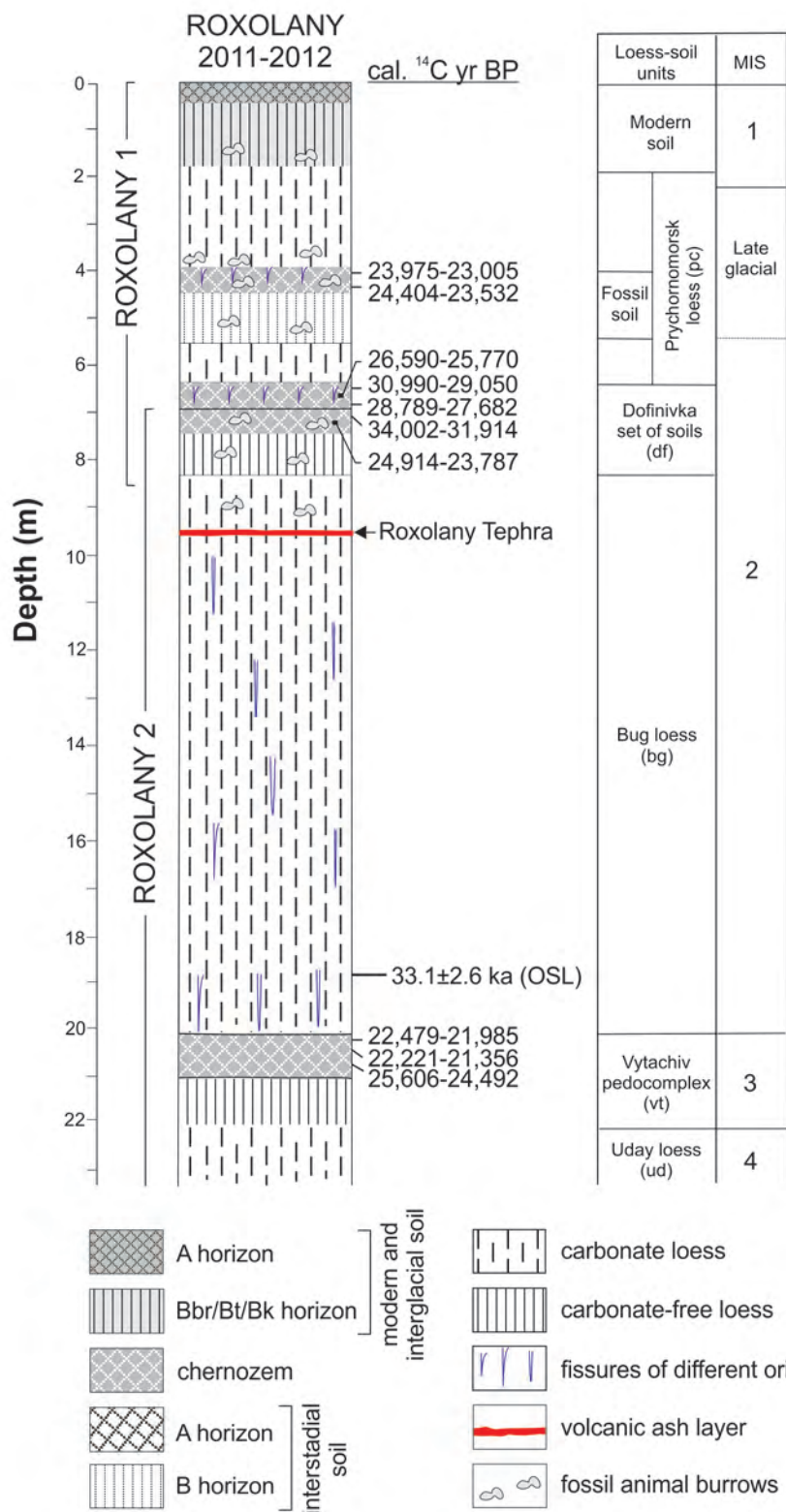


Figure 3

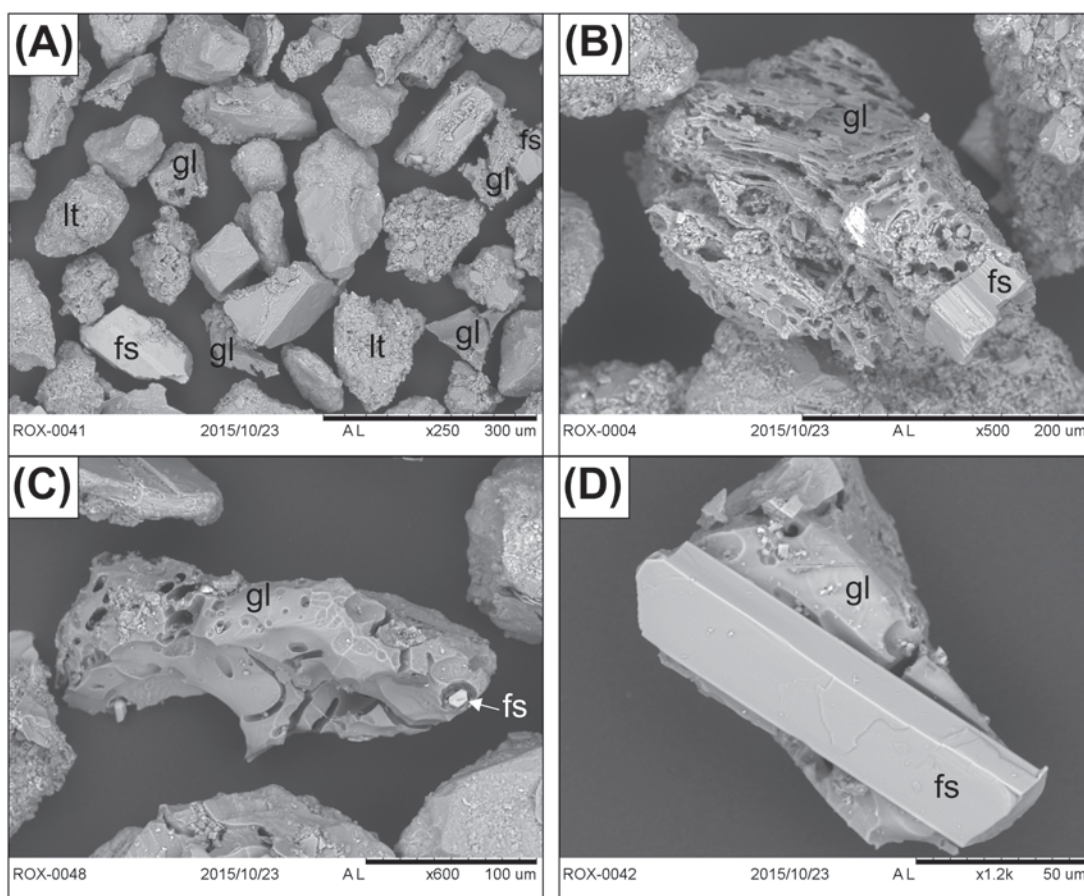


Figure 4

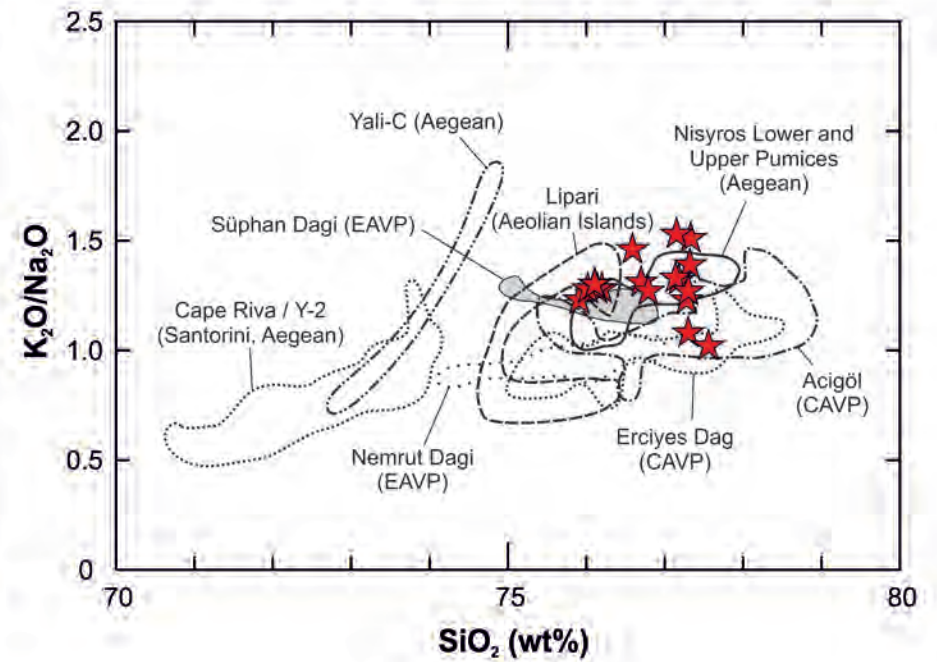
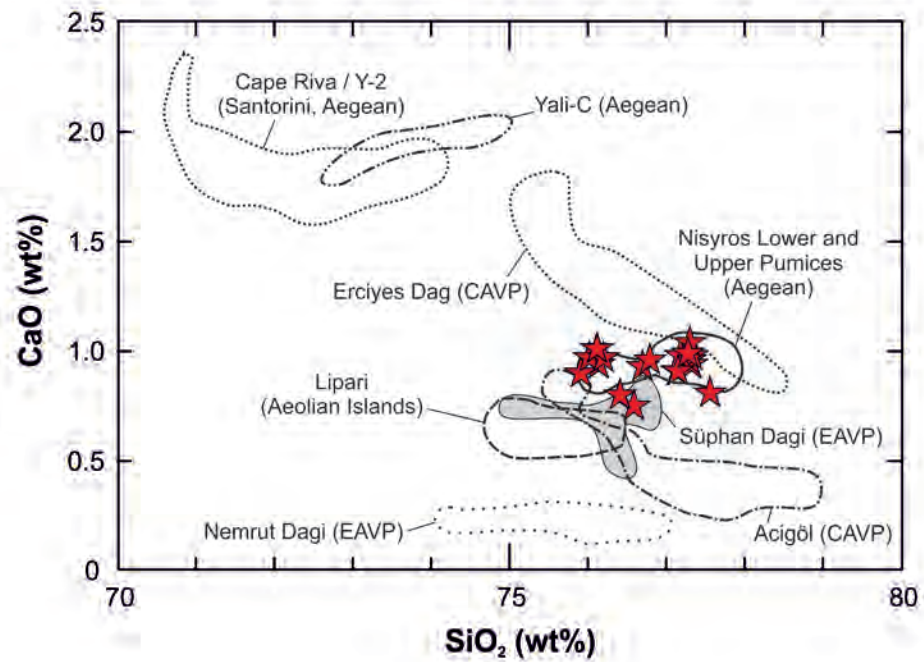
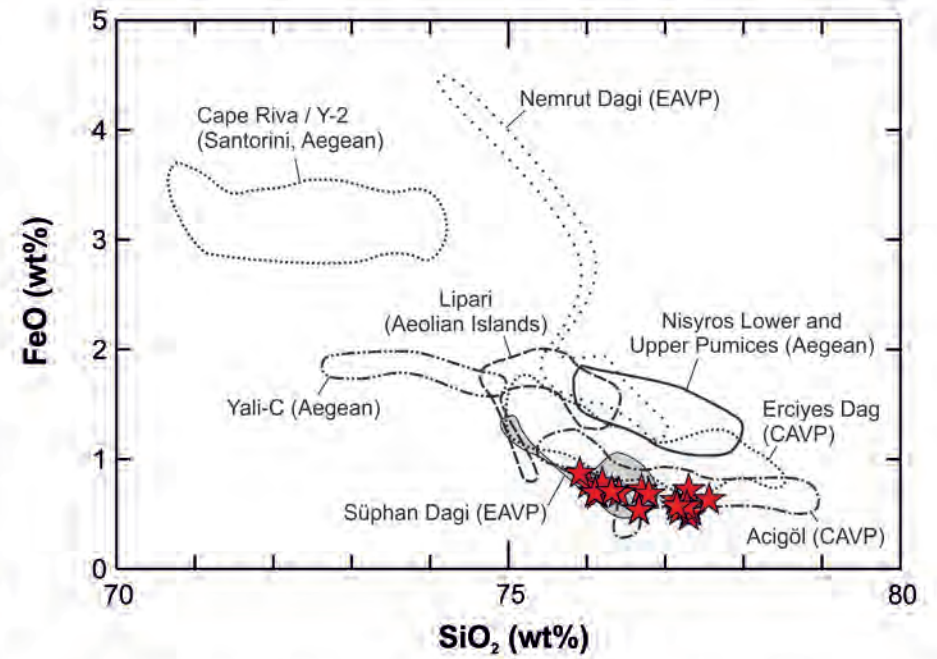
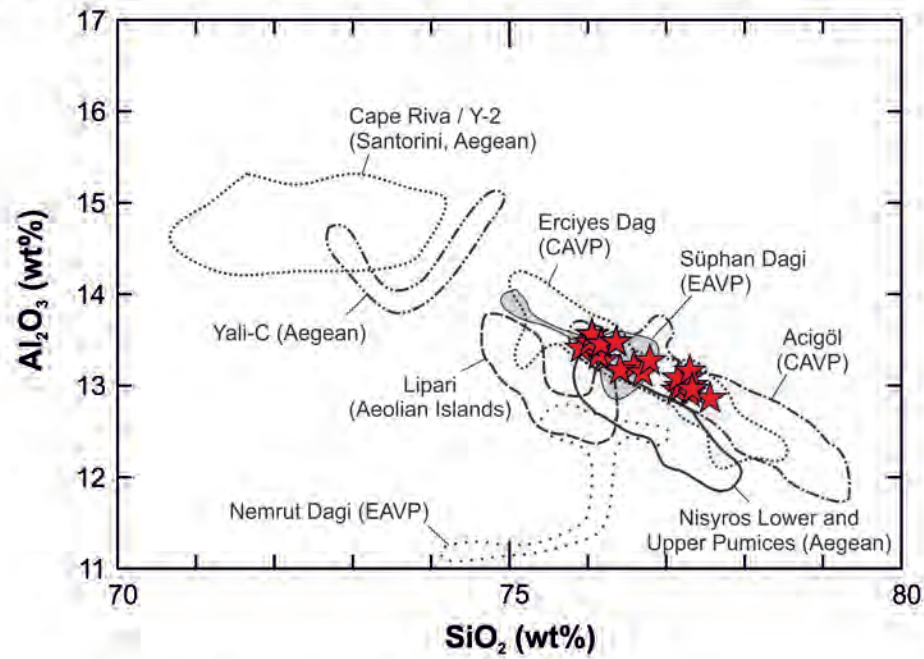


Figure 5

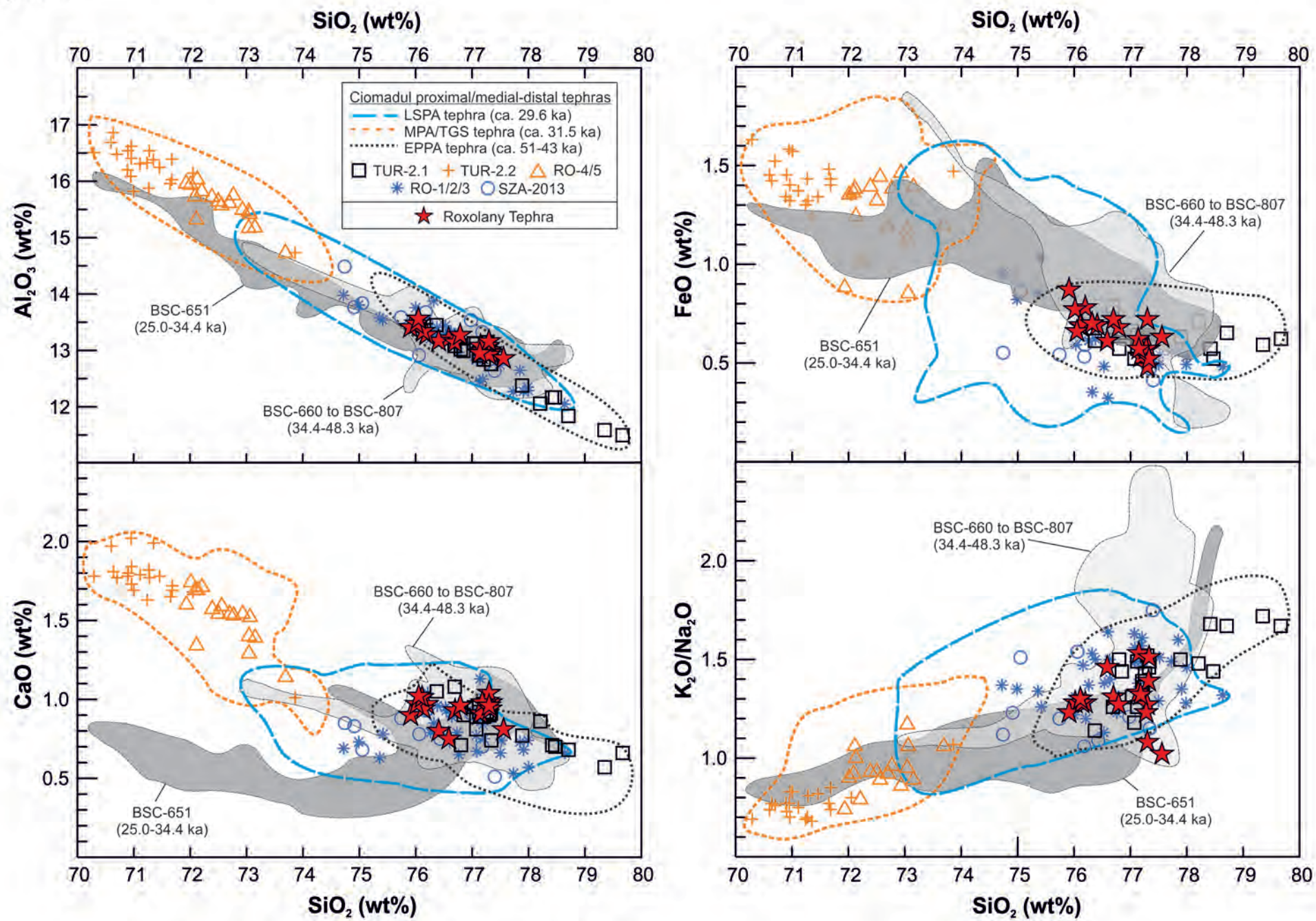


Figure 6

